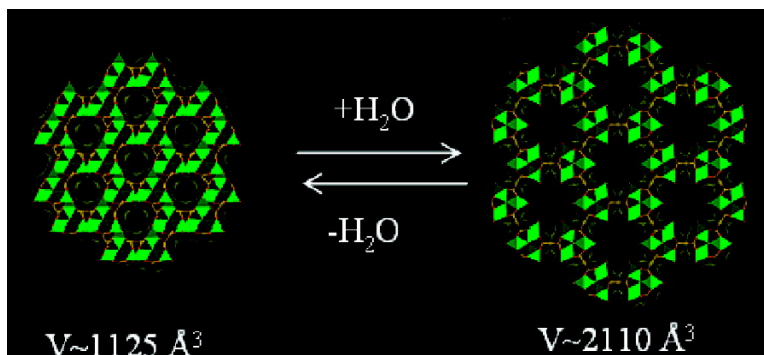


## Very Large Swelling in Hybrid Frameworks: A Combined Computational and Powder Diffraction Study

Caroline Mellot-Draznieks, Christian Serre, Suzy Surbl, Nathalie Audebrand, and Grard Frey

*J. Am. Chem. Soc.*, **2005**, 127 (46), 16273-16278 • DOI: 10.1021/ja054900x • Publication Date (Web): 28 October 2005

Downloaded from <http://pubs.acs.org> on March 25, 2009



### More About This Article

Additional resources and features associated with this article are available within the HTML version:

- Supporting Information
- Links to the 15 articles that cite this article, as of the time of this article download
- Access to high resolution figures
- Links to articles and content related to this article
- Copyright permission to reproduce figures and/or text from this article

[View the Full Text HTML](#)

## Very Large Swelling in Hybrid Frameworks: A Combined Computational and Powder Diffraction Study

Caroline Mellot-Draznieks,<sup>\*,†</sup> Christian Serre,<sup>‡</sup> Suzy Surblé,<sup>‡</sup>  
Nathalie Audebrand,<sup>§</sup> and Gérard Férey<sup>‡,⊥</sup>

*Contribution from the Davy Faraday Research Laboratory, The Royal Institution of Great Britain, 21 Albemarle Street, London W1S 4BS, U.K., Institut Lavoisier, UMR CNRS 8637, Université de Versailles St-Quentin en Yvelines, 45, Avenue des Etats-Unis, 78035 Versailles Cedex, France, Laboratoire de Chimie du Solide et Inorganique Moléculaire, UMR CNRS 6511, Université Rennes I, Avenue du général Leclerc, 35042 Rennes Cedex, France, and Institut Universitaire de France, 103 Boulevard Saint-Michel, 75005 Paris, France*

Received July 21, 2005; E-mail: caroline@ri.ac.uk

**Abstract:** Using a combination of simulations and powder diffraction, we report here the study of the very large swelling of a three-dimensional nanoporous iron(III) carboxylate (MIL-88) which exhibits almost a reversible doubling (~85%) of its cell volume while fully retaining its open-framework topology. The crystal structure of the open form of MIL-88 has been successfully refined and indicates that atomic displacements larger than 4 Å are observed when water or various alcohols are adsorbed in the porous structure, revealing an unusually flexible crystallized framework. X-ray thermodiffraction shows that only a displacive transition occurs during the swelling phenomenon, ruling out any bond breaking.

### Introduction

The rational design of hybrid frameworks is very topical for the applications they imply.<sup>1–5</sup> Their richness lies in the diversity of both framework topologies and properties, which is conveyed in the wide choice of metals combined with a virtually infinite choice of organic counterparts. Among them, the metal carboxylates have emerged as an important family. Di-, tri-, or tetracarboxylates may be used as linkers between inorganic units containing 3d and 4f transition metals,<sup>6–9</sup> providing an effective means of designing novel three-dimensional open frameworks. A few of them exhibit interesting gas storage properties.<sup>6c,7d</sup> In

this research area, the predictability of the framework architectures together with a precise crystal structure determination are essential for an atomic-scale understanding and the possible development of rational design, rendering the use of computational tools essential. However, unlike the case for zeolites and inorganic materials where computational chemistry has a long-standing history,<sup>10</sup> there is a dearth of computational chemistry studies in the area of hybrid frameworks. We have recently developed a series of simulation strategies in the realm of hybrids,<sup>11,12</sup> leading finally to the simulation-assisted chemical structures (SACS) method.<sup>13</sup> For example, this method allowed the computer-assisted structure determination of two three-dimensional chromium carboxylates, MIL-100 and MIL-101,<sup>13,14</sup> revealing complex zeotype architectures with unusually large cells (~380 000 and ~700 000 Å<sup>3</sup>, respectively). We also reported a new type of porous hybrid solids based on trimeric

<sup>†</sup> The Royal Institution of Great Britain.

<sup>‡</sup> Université de Versailles St-Quentin en Yvelines.

<sup>§</sup> Université Rennes I.

<sup>⊥</sup> Institut Universitaire de France.

(1) Férey, G. *Chem. Mater.* **2001**, *13*, 3084.

(2) Feng, S.; Xu, R. *Acc. Chem. Res.* **2001**, *34*, 239.

(3) (a) Eddaoudi, M.; Moler, D. B.; Li, H.; Chen, B.; Reineke, T. M.; O'Keeffe, M.; Yaghi, O. M. *Acc. Chem. Res.* **2001**, *34*, 319–330. (b) Yaghi, O. M.; O'Keeffe, M.; Ockwig, N. W.; Chae, H. K.; Eddaoudi, M.; Kim, J. *Nature* **2003**, *423*, 705.

(4) Rao, C. N. R.; Natarajan, S.; Vaidyanathan, R. *Angew. Chem., Int. Ed.* **2004**, *43*, 1466.

(5) Kitagawa, S.; Kitaura, R.; Noro, S. *Angew. Chem., Int. Ed.* **2004**, *43*, 2334.

(6) (a) Li, H.; Eddaoudi, M.; O'Keeffe, M.; Yaghi, O. M. *Nature* **1999**, *402*, 276–279. (b) Eddaoudi, M.; Kim, J.; Rosi, N.; Vodak, D.; Wachter, J.; O'Keeffe, M.; Yaghi, O. M. *Science* **2002**, *295*, 469. (c) Rosi, N. L.; Eckert, J.; Eddaoudi, M.; Vodak, D. T.; Kim, J.; O'Keeffe, M.; Yaghi, O. M. *Science* **2003**, *300*, 1127. (d) Chae, H. K.; Siberio-Pérez, D. Y.; Kim, J.; Go, Y.; Eddaoudi, M.; Matzger, A. J.; O'Keeffe, M.; Yaghi, O. M. *Nature* **2004**, *427*, 523–527.

(7) (a) Barthelot, K.; Marrot, J.; Riou, D.; Férey, G. *Angew. Chem., Int. Ed.* **2002**, *41*, 281. (b) Serre, C.; Millange, F.; Thouvenot, C.; Noguès, M.; Marsolier, G.; Louër, D.; Férey, G. *J. Am. Chem. Soc.* **2002**, *124*, 13519–13526. (c) Loiseau, T.; Serre, C.; Huguénard, C.; Fink, G.; Taulelle, F.; Henry, M.; Bataille, T.; Férey, G. *Chem. Eur. J.* **2004**, *10*, 1373. (d) Férey, G.; Latroche, M.; Serre, C.; Loiseau, T. *Chem. Commun.* **2003**, 2976–2977. (e) Maspocho, D.; Ruiz-Molina, D.; Wurst, K.; Domingo, N.; Cavallini, M.; Bicarini, F.; Tejada, J.; Rovira, C.; Veciana, J. *Nature Mater.* **2003**, *2*, 190–195.

(8) (a) Livage, C.; Egger, C.; Férey, G. *Chem. Mater.* **1999**, *11*, 1546–1550. (b) Reineke, T. M.; Eddaoudi, M.; O'Keeffe, M.; Yaghi, O. M. *Angew. Chem., Int. Ed.* **1999**, *38*, 2590. (c) Livage, C.; Egger, C.; Férey, G. *Chem. Mater.* **2001**, *13*, 410. (d) Sanselme, M.; Grenèche, J. M.; Riou-Cavellec, M.; Férey, G. *Chem. Commun.* **2002**, 2172.

(9) (a) Serre, C.; Férey, G. *J. Mater. Chem.* **2002**, *12*, 3053. (b) Serre, C.; Millange, F.; Marrot, J.; Férey, G. *Chem. Mater.* **2002**, *14*, 2409. (c) Millange, F.; Serre, C.; Marrot, J.; Gardant, N.; Pellé, F.; Férey, G. *J. Mater. Chem.* **2004**, *14*, 642–645.

(10) *Computer modeling in Inorganic Chemistry*; Catlow, C. R. A., Ed.; Academic Press: San Diego, 1997.

(11) (a) Mellot-Draznieks, C.; Newsam, J. M.; Gorman, A. L.; Freeman, C. M.; Férey, G. *Angew. Chem., Int. Ed.* **2000**, *39*, 2271. (b) Mellot-Draznieks, C.; Férey, G.; Schön, C.; Cancarevic, Z.; Jansen, M. *Chem. Eur. J.* **2002**, *8*, 4102.

(12) (a) Mellot-Draznieks, C.; Dutour, J.; Férey, G. *Angew. Chem., Int. Ed.* **2004**, *43*, 6290–6296. (b) Mellot-Draznieks, C.; Dutour, J.; Férey, G. *Z. Anorg. Allg. Chem.* **2004**, *630*, 2599–2604.

(13) Férey, G.; Serre, C.; Mellot-Draznieks, C.; Millange, F.; Surblé, S.; Dutour, J.; Margiolaki, I. *Angew. Chem., Int. Ed.* **2004**, *43*, 6296.

(14) (a) Férey, G.; Mellot-Draznieks, C.; Serre, C.; Millange, F. *Acc. Chem. Res.* **2005**, *38*, 217. (b) Férey, G.; Mellot-Draznieks, C.; Serre, C.; Millange, F.; Dutour, J.; Surblé, S.; Margiolaki, I. *Science*, in press.

iron(III) subunits.<sup>15</sup> Among them, MIL-88 is a three-dimensional iron(III) fumarate framework,  $\text{Fe}^{\text{III}}_3\text{O}(\text{CH}_3\text{OH})_3\{\text{O}_2\text{C}-\text{C}_2\text{H}_2-\text{CO}_2\}_3\cdot\{\text{O}_2\text{C}-\text{CH}_3\}\cdot 4.5\text{CH}_3\text{OH}$ . Indeed, some possible flexibility of this hybrid framework was observed, indicating a very large swelling capacity upon post-synthesis treatments. However, unlike the case of the carboxylate MIL-53, where the swelling effect upon water adsorption could be structurally studied by standard powder diffraction methods,<sup>6</sup> the low quality of the diffraction patterns of MIL-88 renders the structural characterization of the framework dynamics of MIL-88 untractable using these methods. Thus, in this work, we present a combination of simulations and powder diffraction, which provides valid structural information to describe the unusual flexibility of MIL-88.

### Experimental Section

**As-Synthesized MIL-88.** MIL-88-as (as = as synthesized) was synthesized as described previously.<sup>15</sup> The isolation of MIL-88-as resulted from a controlled secondary building unit (SBU) synthetic approach wherein the inorganic building units—three metallic octahedra shared by  $\mu_3\text{O}$  oxygen atoms—are stabilized in solution prior to further condensation. The resulting three-dimensional framework is built-up from trimers of Fe(III) octahedra linked to fumarate dianions (Figure 1) and exhibits cages together with channels running along the *c* axis. In the as-synthesized solid, both are filled with templating disordered acetate anions and solvent molecules. The full characterization of the crystal structure has shown that the free methanol molecules interact through both hydrogen bonds with oxygens of the inorganic trimers and van der Waals interactions between the free and bound methanol groups. Within the trimeric unit, Fe atoms exhibit an octahedral environment made of four oxygen atoms of the bidentate dicarboxylates, one  $\mu_3\text{O}$  atom ( $\mu_3\text{O}$  represents an oxygen atom connected to three metal centers), and one oxygen atom from the terminal methanol group.

**Post-treatments and X-ray Powder Diffraction.** Starting from MIL-88-as, a series of post-synthesis treatments were performed.

**(1) Drying.** First, the MIL-88-as was dried at 423 K under air, allowing us to evacuate the extraframework species such as methanol molecules.

**(2) MIL-88-Solvents.** The subsequent adsorption of a variety of polar solvents such as  $\text{C}_4\text{H}_9\text{OH}$ ,  $\text{C}_2\text{H}_5\text{OH}$ ,  $\text{CH}_3\text{OH}$ , and  $\text{H}_2\text{O}$  was performed on the dried (423 K) form of MIL-88: a powder sample of dried MIL-88 was dispersed on a glass sample holder and in contact with several solvents. Powder X-ray diffraction data (Figure 2) were collected for sorption characterization of MIL-88-solvent at room temperature on a Siemens D5000 diffractometer using  $\text{Cu K}\alpha$  radiation ( $\lambda = 1.5418 \text{ \AA}$ ) and of MIL-88-dried at 423 K using a Siemens D5005 diffractometer equipped with an Anton Paar HTK1200 high-temperature device.

**(3) MIL-88- $\text{H}_2\text{O}$ .** A powder sample of MIL-88-as was dispersed in water and introduced in a low-absorbing 1 mm diameter glass capillary. X-ray diffraction data were then obtained with a Compagnie Générale de Radiologie powder diffractometer equipped locally with a rotating capillary system and a scintillation detector and using monochromatic  $\text{Cu K}\alpha_1$  radiation ( $\lambda = 1.5406 \text{ \AA}$ ), obtained from an incident-beam quartz monochromator with asymmetric focusing (focal distances 130 and 510 mm), according to an optics described elsewhere (Louër et al. *Adv. X-ray Anal.* **1997**, 40; CD-ROM, Newtown Square, PA; ICDD). The pattern was scanned over the angular range  $5\text{--}50^\circ$  ( $2\theta$ ) with a step length of  $0.025^\circ$  ( $2\theta$ ) and a counting time of  $200 \text{ s step}^{-1}$ . After data collection, the stability of both the X-ray source and the sample was checked by recording again the diffraction lines at low angles. The structure refinement of MIL-88- $\text{H}_2\text{O}$  was performed using Fullprof2k<sup>18</sup> and Winplotr.<sup>19</sup> Fourier differences were performed, using the SHELXTL97 program,<sup>20</sup> to locate the oxygens of the water

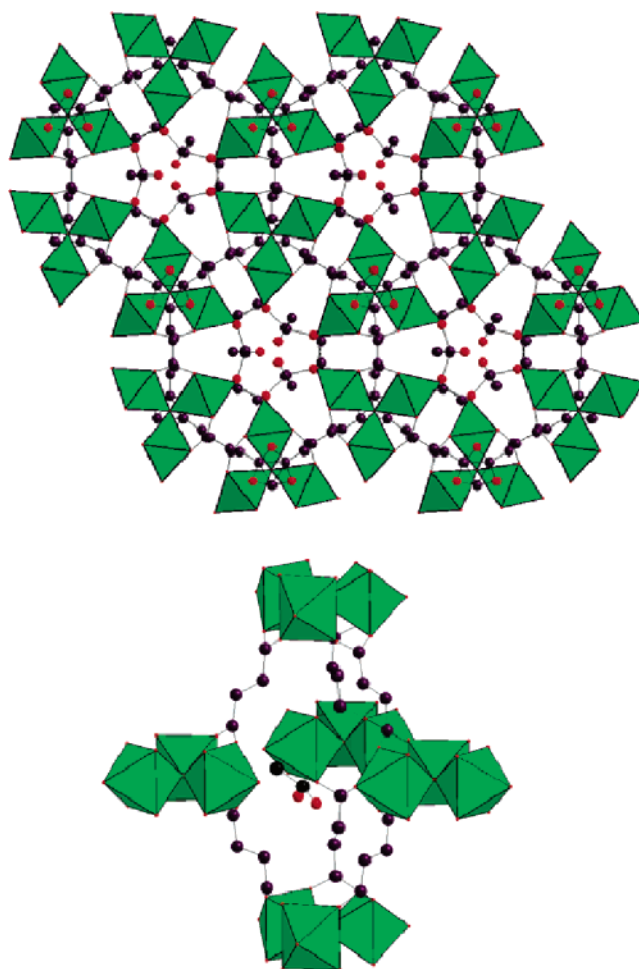


**Figure 1.** Top: Iron-containing trimeric unit extracted from the MIL-88-as crystal structure (view along the *c* axis). Bottom: View of a cage of MIL-88-as crystal structure (only one of the three positions of the disordered acetate is shown for a better understanding). Iron octahedra, oxygen atoms, and carbon atoms are represented in green, red, and black, respectively.

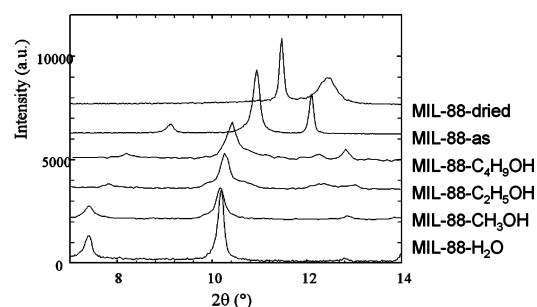


**Figure 2.** Experimental X-ray powder diffraction of MIL-88 ( $\lambda_{\text{Cu}} = 1.5406 \text{ \AA}$ ), dried (423 K), as-synthesized, or wetted with various solvents (alcohols,  $\text{H}_2\text{O}$ ).

molecules in the pores. Crystal data for MIL-88- $\text{H}_2\text{O}$  show a hexagonal space group *P-62c* (No. 190) with  $a = 13.871(1) \text{ \AA}$ ,  $c = 12.663(1) \text{ \AA}$ , and  $Z = 2$  (see Supporting Information for more details).

- (16) *Cerius2*; Accelrys, San Diego, CA, and Cambridge, UK.  
 (17) Rappé, A. K.; Casewit, C. J.; Colwell, K. S.; Goddard, W. A., III; Skiff, W. M. *J. Am. Chem. Soc.* **1992**, *114*, 10024.  
 (18) Rodríguez-Carvajal, J. *FULLPROF: A Program for Rietveld Refinement and Pattern Matching Analysis*, Abstracts of the Satellite Meeting on Powder Diffraction of the XV Congress of the IUCr, p 127, Toulouse, France (1990).  
 (19) Roisnel, T.; Rodríguez-Carvajal, J. *WinPLOTR: a Windows tool for powder diffraction patterns analysis*, Materials Science Forum, Proceedings of the Seventh European Powder Diffraction Conference (EPDIC 7), 2000, Delhez, R., Mittenmeijer, E. J., Eds., pp 118–123.  
 (20) *SHELXL97*; University of Göttingen, Germany, 1997.

(15) Serre, C.; Millange, F.; Surblé, S.; Férey, G. *Angew. Chem., Int. Ed.* **2004**, *43*, 6285–6290.

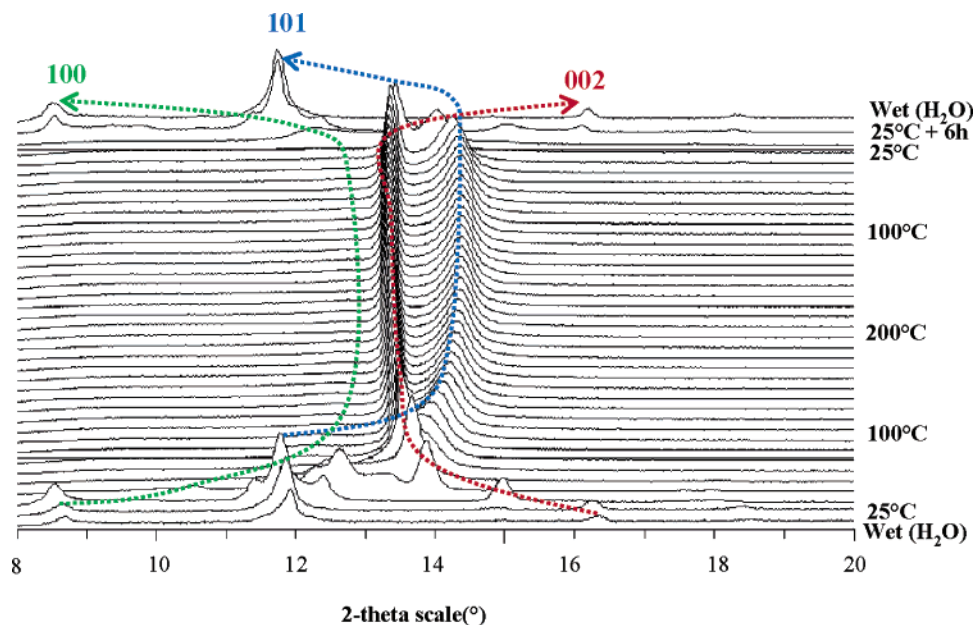


**Figure 3.** X-ray thermodiffractogram ( $\lambda_{\text{Co}} = 1.789007 \text{ \AA}$ ) of MIL-88 under air atmosphere starting from the MIL-88- $\text{H}_2\text{O}$  solid at room temperature. At the end of the experiment, back at room temperature, the powder is wet again with water and an X-ray diffraction pattern is collected. For a better understanding, the evolution of the positions of the Bragg 100 (green), 101 (blue), and 002 (red) reflections is followed by colored arrows on the pattern.

**Thermodiffraction.** To accurately follow the structural changes accompanying the drying process in the MIL-88-as sample, additional X-ray thermodiffractometry was performed in the furnace of a Siemens D-5000 diffractometer in the  $\theta$ - $\theta$  mode under air ( $\lambda_{\text{Co}} = 1.789007 \text{ \AA}$ ). A fresh sample of MIL-88-as was first dispersed on the platinum sample holder and wetted with deionized water. The sample was then heated slowly to 200 °C and cooled to room temperature. Finally, the resulting powder was wetted again with water, and an additional X-ray pattern was collected. Each pattern was recorded within the 7–35° ( $2\theta$ ) range with 2 s  $\text{step}^{-1}$ , which gave an approximate 1 h length for each pattern at the corresponding temperature. The heating rate between two temperatures was 5 °C/min.

### Computational Section

To assess the structural modifications of MIL-88 upon drying and solvent adsorption, a computer simulation approach was applied. Indeed, we aimed at extracting from the experimental data (cell parameters, diffraction pattern) a viable atomic-scale description of the swelling, yielding a simulated crystal structure for the dried MIL-88 and for each type of MIL-88-solvent solid. The simulations were performed only on the MIL-88 framework as follows. An initial model for the framework was computationally built from the experimental as-synthesized structure, MIL-88-as ( $a = 11.18 \text{ \AA}$ ,  $c = 14.68 \text{ \AA}$ ,  $P-62c$ ),<sup>15</sup> not taking the extraframework species into account. The second step consisted of energy-minimizing the hybrid framework in  $P-62c$ , relaxing atomic coordinates and cell parameters in the following sequential fashion: the key feature of this step lies in the use of carefully chosen external constraints along the cell axes (i.e., hydrostatic pressure) so as to enforce the elongation or the shrinkage of the crystal structure along specific cell axes during the energy minimizations. The hydrostatic pressure is therefore applied anisotropically, for example along  $a$  while keeping  $c$  fixed or vice versa. This pressure is chosen as positive when a shrinkage along a cell axis is required or negative in the case of an elongation. The model of MIL-88-as is energy-minimized sequentially; i.e., the anisotropic hydrostatic pressure is adjusted at each minimization step until the simulated cell parameters match the experimental ones. This way, the flexible hybrid framework is enforced to adopt the targeted experimental cell parameters while retaining its network's connectivity. The simulations were done with the Cerius2 suite of software<sup>16</sup> and the universal force field with periodic boundary

conditions.<sup>17</sup> The force field is used as a simple means to ensure that the so-minimized hybrid frameworks are realistic, i.e., kept within an acceptable range of structural features (bond distances, angles, etc.).

While electrostatic interactions are indeed believed to play an important role in the dynamics of the swelling, especially with the adsorption of polar molecules, electrostatic interactions were not computed in this work. Future investigations will be undertaken to determine individual charges on both the hybrid framework and solvent molecules and elucidate their role in the dynamics of the “breathing”. Therefore, the simulation results presented here are only meant to yield a qualitative structural picture of the swelling.

### Results and Discussion

The as-synthesized structure showed an unusual flexibility upon drying treatments and adsorption of polar solvent molecules. The X-ray powder pattern of the dried (423 K) form of MIL-88, i.e., free of extraframework water and organic solvent molecules, seems significantly different from that of the parent (Figure 2). Also, the four solids that result from the subsequent adsorption of a variety of polar solvents ( $\text{H}_2\text{O}$ ,  $\text{CH}_3\text{OH}$ ,  $\text{C}_2\text{H}_5\text{OH}$ , and  $\text{C}_4\text{H}_9\text{OH}$ ) in the dried MIL-88 are intriguingly different from the initial dried form (Figure 2). In all cases, the uptake is fast and fully reversible with temperature as shown by thermodiffraction, as exemplified in Figure 3 for water adsorption. The indexing of the five powder patterns, labeled MIL-88-dried, MIL-88- $\text{H}_2\text{O}$ , MIL-88- $\text{CH}_3\text{OH}$ , MIL-88- $\text{C}_2\text{H}_5\text{OH}$ , and MIL-88- $\text{C}_4\text{H}_9\text{OH}$ , interestingly shows that all structures exhibit the same symmetry (hexagonal) and space group ( $P-62c$ ) as the parent MIL-88-as. This obviously suggests that the topology of the framework is maintained while being submitted to a very large swelling effect. The drying leads to the contracted form while the hydration yields the most open form. The uptake of solvent by the dried phase is very fast, within a few seconds at room temperature.

This is further evidenced by the impressive evolution of the cell parameters and volumes (Table 1) with drying and adsorption of polar solvent molecules. The drying at 423 K of MIL-

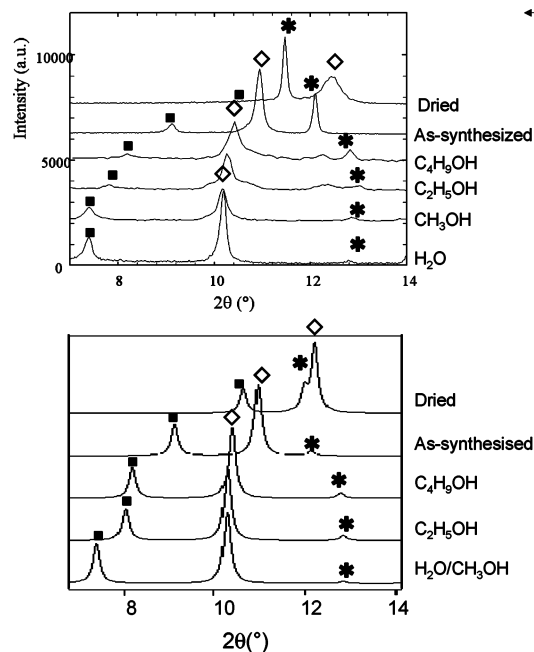


**Figure 4.** Simulated diffraction patterns of MIL-88-dried (423 K) or wetted with various solvents (alcohols, H<sub>2</sub>O). For a better understanding, the corresponding experimental X-ray patterns ( $\lambda_{\text{Cu}} = 1.5406 \text{ \AA}$ ) are shown at the top of the figure.

88-as ( $V = 1580 \text{ \AA}^3$ ) evacuates the extraframework species. The result is an important shrinkage of the cell volume ( $\sim 25\%$ ), mainly due to a decrease in the  $a$  parameter. Still, this contraction is quite unexpected in comparison with the chro-

**Table 1.** Cell Parameters of the MIL-88 Structures

type of post-treatment	$a$ (Å)	$c$ (Å)	volume (Å <sup>3</sup> )
dried at 423 K	9.26	15.31	1135
<b>as-synthesized (dried at RT)</b>	<b>11.18</b>	<b>14.59</b>	<b>1580</b>
adsorption of C <sub>4</sub> H <sub>9</sub> OH	12.46	13.70	1840
adsorption of C <sub>2</sub> H <sub>5</sub> OH	13.07	13.30	1970
adsorption of CH <sub>3</sub> OH	13.78	12.69	2090
adsorption of H <sub>2</sub> O	13.87	12.66	2110

mium or aluminum terephthalates MIL-53, where a very large opening of the structure is observed upon drying instead.<sup>7b,c</sup>

The room-temperature adsorption of the different alcohols and water into MIL-88-dried induces an increase in the cell volumes, inversely proportional to the mass of the solvent molecule. The largest swelling occurs in the hydrated form, where the  $a$  parameter gradually increases ( $9.26 \rightarrow 13.87 \text{ \AA}$ ), while the  $c$  parameter decreases concomitantly to a lesser extent ( $15.31 \rightarrow 12.66 \text{ \AA}$ ). The cell volume increases by  $\sim 85\%$  from the contracted ( $1135 \text{ \AA}^3$ ) to the open form of MIL-88-H<sub>2</sub>O ( $2110 \text{ \AA}^3$ ). Such flexibility suggests that the channels may be contracted when empty and re-opened in the presence of the polar solvent molecules, with the creation of hydrogen bonds between solvent molecules themselves and with the organic framework. At this point, the question is whether bond breaking occurs during the swelling. The thermodiffraction (Figure 3) shows a continuous evolution of the pattern during the exchange, which indicates that the process is not reconstructive but only displacive, which is known not to break any bond. We believe that if the swelling were reconstructive, the X-ray patterns would show the coexistence of the two phases in a

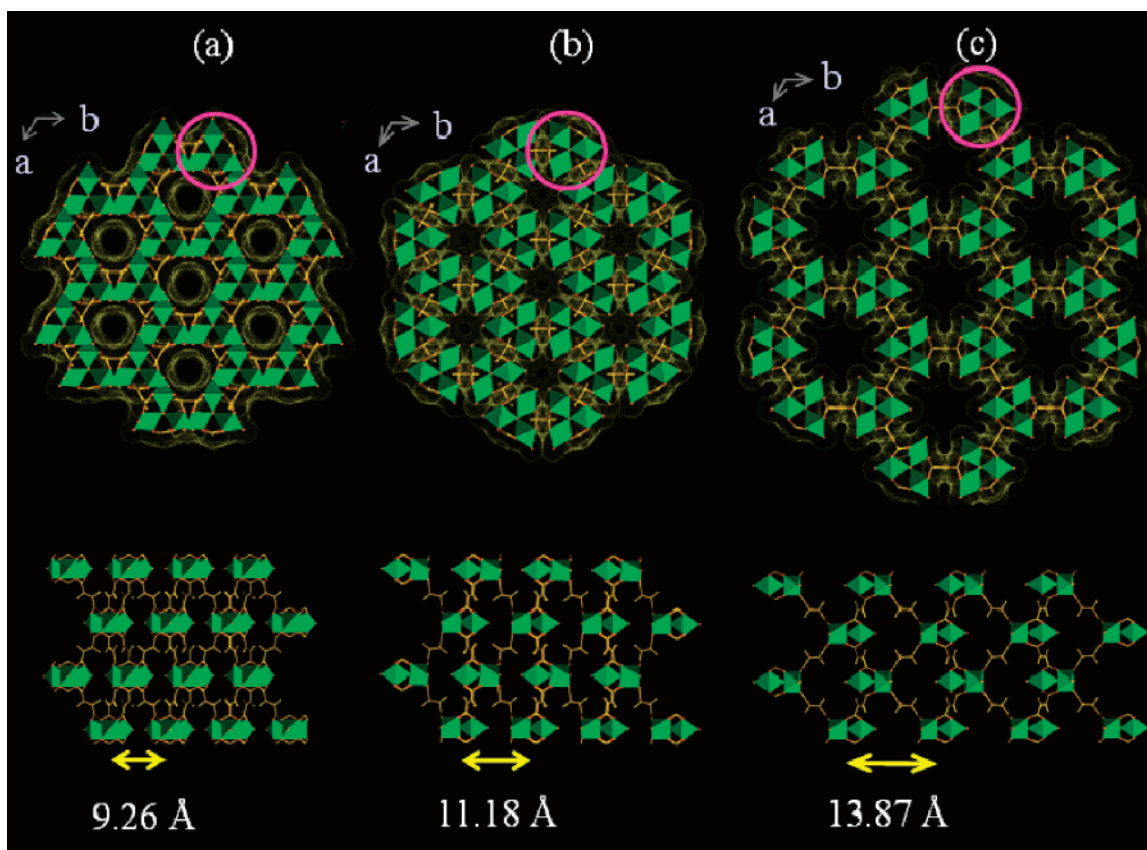


**Figure 5.** Simulated crystal structures of the MIL-88 framework in its contracted (a), as-synthesized (b), and open (c) forms. It is noteworthy that the  $a$  cell parameter increases gradually from one structure to the next, as a direct measure of distance between the inorganic trimeric units and of the amplitude of the swelling. The Connolly surface of each structure is shown in yellow.

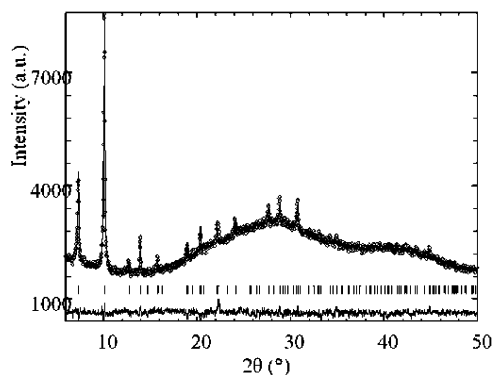


**Figure 6.** Rietveld plot of MIL-88-H<sub>2</sub>O ( $\lambda_{\text{Cu}} = 1.5406 \text{ \AA}$ ).

certain range of temperatures. This is not observed, therefore suggesting that this very large swelling phenomenon occurs without bond breaking while fully retaining the topology of the framework.

Typically, to simulate the contracted cell of MIL-88-dried ( $a_{\text{final}} = 9.26 \text{ \AA}$ ), a positive hydrostatic pressure was first applied along the  $a$  axis when minimizing the MIL-88-as model ( $a_{\text{initial}} = 11.18 \text{ \AA}$ ), while keeping the  $c$  parameter fixed. In a second step, a small negative hydrostatic pressure was applied along  $c$  ( $c_{\text{initial}} = 15.24 \text{ \AA}$ ), while keeping  $a$  fixed, to converge toward the larger expected value ( $c = 15.31 \text{ \AA}$ ). A similar approach was applied to simulate the crystal structure of each of the expanded cells of MIL-88, using one minimized structure as a starting model for the following larger structure. All models converged relatively easily toward the experimental cell parameters while maintaining the framework topology within realistic structural features. Finally, the powder diffraction patterns of the different versions of MIL-88 were simulated and their consistency was checked against the experimental patterns (Figure 4). Indeed, the calculated patterns of the series of simulated MIL-88 crystal structures reproduce with a relatively good agreement the experimental trend of the diffraction patterns in terms of Bragg positions, with however significant differences in Bragg intensities due to the absence of the extraframework species in the simulations. In particular, the simulations reproduce very well the lower angle shift of the (002) Bragg reflection together with the high angle shift of the (101) reflection, both reflections finally showing an important overlap in the dried phase.

Figure 5 shows a selection of the simulated crystal structures of MIL-88- $n$  covering the whole range of swelling, i.e., its contracted form (Figure 5a) and the hydrated open form (Figure 5c) compared to the framework of the as-synthesized crystal structure (Figure 5b). During the simulations, a rotation of trimeric units apart from each another is observed, which is allowed by the natural flexibility of the organic  $\text{O}_2\text{C}-\text{C}_2\text{H}_2-\text{CO}_2$  carboxylate molecules: a free rotation of the COO groups around the C–C single bond together with a change in the dihedral angle between the COO plane and the Fe–Fe–Fe planes defined within the trimers. A careful inspection of the structure suggests that the swelling of the framework derives not only from the above two degrees of freedom of the trimers and of the COO groups toward the double bond of the carbon chain, but also from the absence in the bipyramid of any linkage between its “equatorial” trimers via fumarate anions in the (001) plane. If this linkage had existed, the bipyramid would have fumarate rigid bonds between all the trimers of the structure,

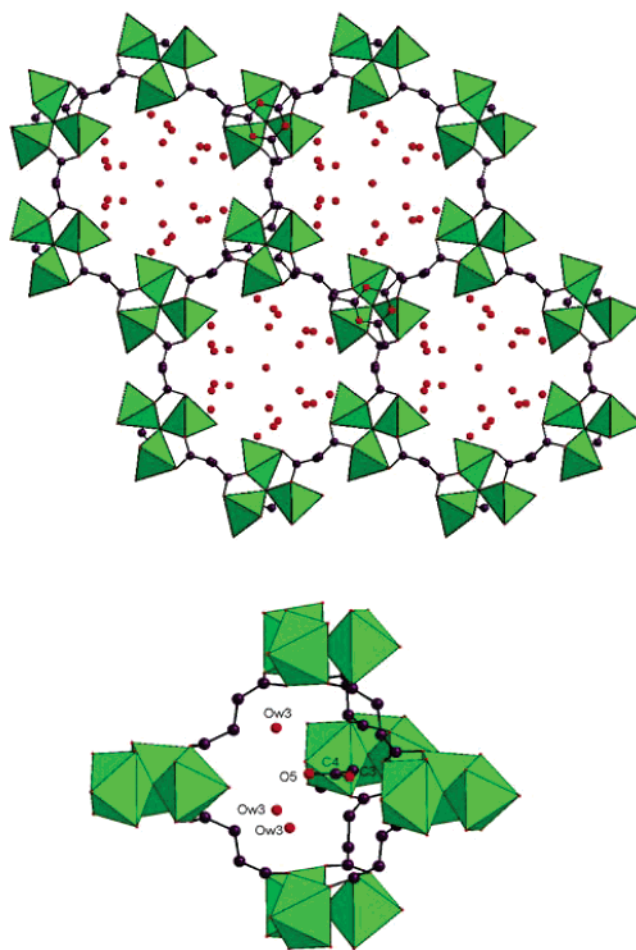


**Figure 7.** Top: View of the crystal structure of MIL-88-H<sub>2</sub>O along the  $c$  axis. Bottom: View of a cage of MIL-88-H<sub>2</sub>O (only one of the three positions of the disordered acetate C(3), C(4), and O(5) is shown for a better understanding). Iron octahedra, oxygen atoms, and carbon atoms are represented in green, red, and black, respectively.

corresponding to the edges of the bipyramid and therefore creating triangular cycles of trimers which are well known for conferring a strong rigidity to the edifices. The absence of such linkages provides freedom for the distances between the “equatorial” trimeric units of the (001) planes. This distance is minimum for MIL-88-dried and maximum for MIL-88-H<sub>2</sub>O. It can be directly measured as the value of the  $a$  cell parameter, which represents the  $\mu_3\text{O}-\mu_3\text{O}$  distances between neighboring trimers lying in (001):  $9.26 \text{ \AA}$  in the dried form,  $11.18 \text{ \AA}$  in MIL-88-as, and  $13.87 \text{ \AA}$  in the hydrated open structure. The correlative change in the  $c$  parameter reflects the evolution of the height of the bipyramid.

To check the validity of the simulation data, high-quality X-ray powder diffraction data were collected—using a rotating capillary tube—on MIL-88-H<sub>2</sub>O, i.e., the most open version, and the crystal structure simulated above was used as a starting model for the Rietveld refinement of the diffraction pattern. Fourier difference maps were used to locate water molecules. Indeed, a successful refinement was performed (Figure 6), and the refined crystal structure reveals a slight distortion and some tilting of the inorganic trimers in comparison with the initial simulated model, probably as a result of the presence of the polar water molecules, which were not taken into account in the simulations (Figure 7). A large number of free water

molecules were located (38 H<sub>2</sub>O/unit cell, or 6.33 H<sub>2</sub>O/Fe) leading to the formula Fe<sup>III</sup><sub>3</sub>O(H<sub>2</sub>O)<sub>3</sub>{<sup>-</sup>O<sub>2</sub>C-C<sub>2</sub>H<sub>2</sub>-CO<sub>2</sub><sup>-</sup>}<sub>3</sub>·{<sup>-</sup>O<sub>2</sub>C-CH<sub>3</sub>}·19H<sub>2</sub>O. Assuming a ~20 Å<sup>3</sup> volume per water molecule, the volume occupied by both free and bound water molecules is estimated to be ca. 880 Å<sup>3</sup>, which is consistent with the cell volume expansion observed between the dried and hydrated forms. Almost 30% of the free water molecules (Ow-(3)) are located within the narrow bipyramidal cages delimited by five trimers (see Figure 7) interacting with the acetate counteranions. We believe that these cages may admit small and polar molecules such as water or methanol more easily than larger hydrophobic alcohols, which may explain the differences in the amplitude of swelling from one alcohol to another.

### Conclusion

The unusually large swelling of the iron fumarate MIL-88 shows how the response of the hybrid framework is very dependent upon both the type of metal-organic connectivity (including the flexibility of the carboxylate ligand) and the nature of the extraframework species, depending on the size and the polarity of the organic molecule involved. MIL-88 represents an illustrative example of a highly flexible hybrid network involving cooperative atomic displacements larger than 4 Å upon adsorption of various solvents (H<sub>2</sub>O, CH<sub>3</sub>OH, C<sub>2</sub>H<sub>5</sub>-OH, C<sub>4</sub>H<sub>9</sub>OH). Unlike zeolitic materials that are characterized

by a relatively rigid framework under adsorption conditions, such flexible frameworks may offer the advantage of performing the adsorption of a wide range of organic molecules or gases in a more specific fashion by simply adapting its framework structure accordingly. A deeper atomic-scale understanding of such a mechanism is certainly needed. While this study shows the efficiency of a combined computational-diffraction approach for yielding a detailed atomic-scale description of the swelling properties of this class of solids, further work is in progress in order to elucidate the role of the solvent molecules at the interface between extraframework species and the hybrid framework where specific short-range interactions may be at play.

**Acknowledgment.** Gérard Marsolier from Laboratoire de Chimie du Solide et Inorganique Moléculaire, Rennes, France, is acknowledged for his help in collecting the X-ray diffraction pattern of MIL-88-H<sub>2</sub>O.

**Supporting Information Available:** Crystal data, structural refinement parameters, and crystal structure of MIL-88-H<sub>2</sub>O. This material is available free of charge via the Internet at <http://pubs.acs.org>.

JA054900X